Kinetics Study of Slurry-Phase Propylene Polymerization with Highly Active $Mg(OEt)_2$/Benzoyl Chloride/$TiCl_4$ Catalyst

IL KIM,* HONG KI CHOI, JAE HA KIM, and SEONG IHL WOO†

Department of Chemical Engineering, Korea Advanced Institute of Science and Technology, 373-1, Kusong-Dong, Yusong-Ku, Taejon, South Korea

SYNOPSIS

Propylene was polymerized in a slurry phase over superactive and stereospecific catalyst prepared by the reaction of $Mg(OEt)_2$ with benzoyl chloride and $TiCl_4$ in the presence of $AlEt_3$ with or without an external donor. A kinetic analysis of propylene polymerization was carried out. The polymerization rate was first order with respect to monomer concentration and the dependence of overall polymerization rate on the concentration of $AlEt_3$ can be explained by the Langmuir adsorption mechanism. Maximum activity was observed around an Al/Ti mole ratio of 20. The average rate over 90 min of polymerization as a function of temperature showed a maximum around 42°C and the overall activation energy was 8.5 kcal/mol at $T < 42$°C and −4.0 kcal/mol at $T > 42$°C. The analysis of the phenomenon of an optimum temperature gave 2.2 kcal/mol for the activation energy of the rate-determining step, and 6.3 kcal/mol, for the adsorption energy of $AlEt_3$. The addition of small amount of *p*-ethoxyethyl benzoate (PEEB) as an external donor increased the percentage of isotactic polymer to 98% and slightly increased activity in spite of the decrease in the concentration of active centers due to the stabilizing effect of the active centers by the external donor. The temperature showing maximum yield was shifted to the higher temperature when $AlEt_3$ and PEEB ($[AlEt_3]/[PEEB] = 5$) was used as a cocatalyst.

INTRODUCTION

Highly active Ziegler–Natta catalysts obtained by combining a component comprising a magnesium compound and a titanium compound with an activating organoaluminum compound were reported about 20 years ago and have gained significant industrial importance in recent years because the improved activity has eliminated catalyst removal procedures after polymerization.[1-3] The polymerization activity and the stereospecificity of these catalysts can be improved by incorporating an electron donor (Lewis base) into the catalyst component.

During the preparation of this type of catalyst, various kinds of magnesium compounds such as $MgCl_2$, $Mg(OH)Cl$, MgR_2, $Mg(OR)_2$, $Mg(OH)_2$, and Mg powder may be used as a starting substance for a support.[1,2] These magnesium compounds can be transformed into $MgCl_2$ by $TiCl_4$ and organic compound-containing halogens. The halogenation of magnesium dialkoxides or diaryloxides by reacting with titanium tetrachloride in the presence of an inert hydrocarbon solvent has been proposed in the patent literature.[4] These halogenated reaction products may be modified by reacting further with an electron donor. More improved catalysts of this type and processes for olefin polymerization were disclosed by Shell Oil Co.[5,6] These catalysts are prepared by halogenating a magnesium compound $MgR'R''$ (wherein R′ and R″ are alkyl, aryl, alkoxide, or aryloxide groups and R″ may also be a halogen) by reaction with a halide of tetravalent titanium in the presence of an electron donor and a halohydro-

* Present address: Department of Chemical Engineering, University of Ulsan, P.O. Box 18, Ulsan, Kyungnam 680-749, South Korea.

† To whom correspondence should be addressed.

Journal of Applied Polymer Science, Vol. 52, 1739–1750 (1994)
 CCC 0021-8995/94/121739-12

carbon, followed by further contact of the halogenated product with a tetravalent titanium compound.

In a previous article, we described detailed steps to prepare one of this type of catalyst obtained by reacting $Mg(OEt)_2$ with $TiCl_4$ and benzoyl chloride (to generate ethyl benzoate [EB] *in situ*) in the presence of chlorobenzene and investigated polymerization rate profiles, chemical compositions, and the reaction among $TiCl_4$, $Mg(OEt)_2$, benzoyl chloride, and chlorobenzene by using FTIR and quantitative analysis of Lewis base, BET, thermal analysis, and X-ray diffraction.[7] Through the determination of the number of active centers for propylene and ethylene polymerization with this catalyst, it was found that this type of catalyst had more active sites than that of a $MgCl_2$-supported highly active catalyst or conventional Ziegler–Natta catalysts.[8]

In this article, semibatch polymerization tests were performed in *n*-heptane slurry under constant propylene pressure to investigate the kinetic behavior of the catalyst.

EXPERIMENTAL

Materials

Extrapure heptane (from Tedia Co., USA) and hexane (from Duksan Pharmaceutical Co., South Korea) were dried over sodium and fractionally distilled before use. A solution of benzoyl chloride (PhCOCl, from Kanto Chemical Co., Japan) in benzene was washed with 5% $NaHCO_3$ cold solution, separated, dried with $CaCl_2$, and distilled. Chlorobenzene (PhCl, from Kanto Chemical Co.) was purified by the same method as was PhCOCl and passed through a Linde 4 Å molecular sieve column. *p*-Ethoxyethyl benzoate (PEEB, from Aldrich, USA) and phenyltriethoxysilane (PTES, from Aldrich) were diluted with anhydrous heptane before use. $Mg(OEt)_2$ (from Strem Chemical Co., USA), $AlEt_3$ (from Aldrich), and $TiCl_4$ (from Kanto Chemical Co.) were used as received.

Preparation of Catalyst

A Schlenk-type reactor (300 mL) equipped with a fritted disc (ASTM 10–15) was used to prepare the catalyst. The reactor was first dried for 1 day above 150°C and introduced into dry box to put the exact amount of $Mg(OEt)_2$ into the reactor. The reactor was designed to facilitate hot filtration, washing, and reaction with additional $TiCl_4$, with or without PhCOCl.

$Mg(OEt)_2$ (50 mmol) was stirred at 100°C with PhCOCl (15.6 mmol) and 75 mL of PhCl as $TiCl_4$ (75 mL) was added dropwise for 20 min. The mixture was brought to 100°C and stirred for 180 min, then filtered hot. The hot-filtered solid product was slurried in 75 mL of PhCl and held at 100°C for 120 min, then filtered hot. Again, the hot-filtered solid was slurried in $TiCl_4$ (50 mL) containing 5.2 mmol of PhCOCl and reacted at 100°C for 120 min, then filtered hot. The greenish solid was washed with 150 mL of boiling *n*-hexane seven times and stored under *n*-heptane for the polymerization.

Polymerization

Slurry-phase polymerization of propylene was carried out in a 250 mL glass reactor. A Teflon magnetic spinbar was used for the agitation. First, 100 mL of heptane containing the prescribed amount of $AlEt_3$ was introduced into the reactor; the nitrogen was then pumped off and the reactor was flushed out with monomer. After raising the temperature to a desired point, propylene was saturated into the heptane solvent. When no more absorption of propylene into heptane was observed, a prescribed amount of catalyst slurry was introduced into the reactor by a tuberculin syringe and then the polymerization was started. To obtain reproducible results (within ±5%), it was essential to prepare polymerization mixtures in an identical manner. All the components of polymerization were made up in a similar manner and mixed in the same order. The polymerization reactor setup is shown in Figure 1.

The polymerization mixture was stirred at the speed of 1600 rpm to avoid the effect of monomer diffusion through the gas–liquid interface. The temperature of polymerization was controlled within ±0.1°C. The polymerization rate was determined at every 0.01 s from the rate of propylene consumption, measured by a hot-wire flowmeter (Model 5850D from Brooks Instrument Div.) connected to a personal computer through a A/D converter. The polymer yield estimated from the consumption rate of propylene agreed within ±5% with the actual yield measured by the weight of polymer after polymerization. A known amount of CO was injected into the polymerization reactor through a gas-tight syringe and the decrease in the overall rate of polymerization was measured simultaneously to determine the number of active centers.[8,9]

Analysis

The nascent morphology of the catalyst was examined using a scanning electron microscope (SEM)

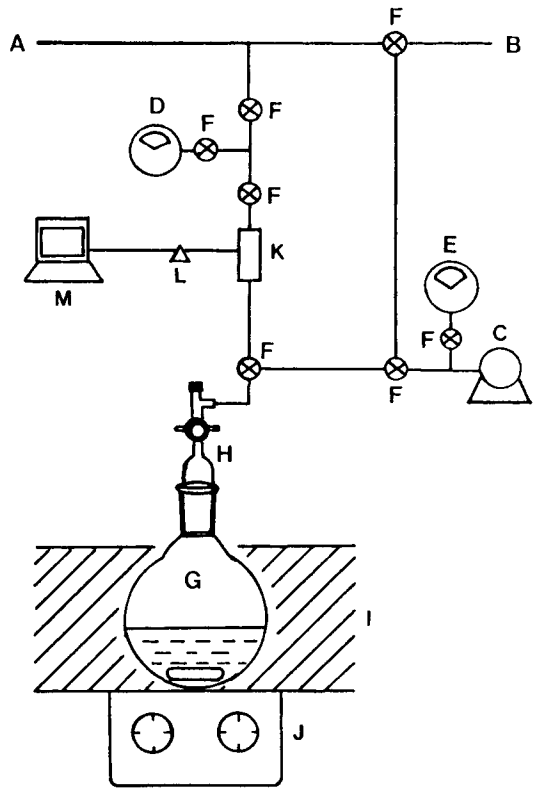

Figure 1 Propylene polymerization setup: (A) monomer inlet; (B) nitrogen inlet; (C) vacuum pump; (D) pressure gauge; (E) vacuum gauge; (F) valves; (G) reactor; (H) septum inlet adapter; (I) constant temperature bath; (J) magnetic stirrer; (K) mass flowmeter; (L) A/D converter; (M) personal computer.

technique under an inert atmosphere. The selectivity to isotactic polypropylene was determined by measuring the amount of xylene soluble (XS) material. About 2 g of sample was placed in the thimble of a Soxhlet extractor with about 100 mL of xylene and subjected to extraction under reflux of the boiling xylene for 16 h. The amount of polymer dissolved in the xylene was determined after evaporating xylene and further drying the residue in a vacuum oven at 80°C for 16 h. The magnitude of XS in the case of propylene homopolymer is typically about 2% greater than the amount of polymer extractable in refluxing *n*-heptane.[6] Thus, the isotacticity index (I.I.) of polypropylene (amount insoluble in refluxing *n*-heptane) is approximately 100 − (XS − 2).

RESULTS AND DISCUSSION

Elimination of Diffusional Effects

Since there are a number of different processes in heterogeneous Ziegler–Natta polymerization that can interfere with each other in different ways, it is necessary to find a kinetically controlled polymerization condition. For the study of the kinetics of slurry-phase olefin polymerization at steady-state conditions, the elimination of physical effects (e.g., heat and mass transfer) in the polymerization reactor is very important.[10] To avoid this effect, we estimated the effect of monomer diffusion on the polymerization rate $[(dR_p/dt)_0]$ extrapolated to the beginning of the reaction by changing the rotating speed of the stirrer.[11] Figure 2 shows that the initial rate, $(dR_p/dt)_0$, becomes constant and independent of the stirring speed above 750 rpm. At this stirring speed, the absorption rate of monomer through the *n*-heptane solvent to the polymerizing particles is larger than the rate of polymerization, indicating that there is a stationary monomer concentration in the solvent. Hence, all the polymerizations were carried out at the stirring speed of 1600 rpm. For reproducible kinetic results, it is essential to maintain the amount of polymer in *n*-heptane less than 33% by volume. This indicates that 100 mL of *n*-heptane solvent may contain at most 15 g polymer with a bulk density of 0.4 g/cm^3.

In slurry-phase olefin polymerization, it is very important to determine whether polymerization is diffusion-controlled by measuring the polymerization rate with different amounts of catalyst. Figure 3 shows the first-order dependency of R_p on the amount of catalyst. As the amount of catalyst was doubled and tripled, the maximum rate $(R_{p,m})$ increased as much as 2.1 and 3.1 times, respectively, and the corresponding average polymerization rate over 60 min of polymerization $(R_{p,60\ \mathrm{min}})$ increased

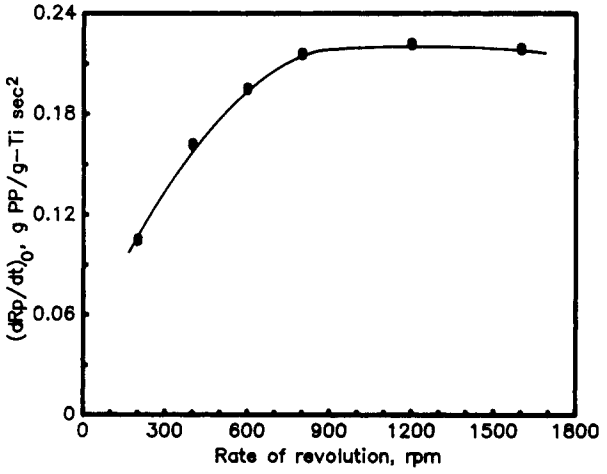

Figure 2 Initial rate, $(dR_p/dt)_0$, as a function of the stirring speed. Polymerization conditions: T = 50°C; $[C_3H_6]$ = 0.43M; Ti = 4.1 × 10^{-4} g; $[AlEt_3]$ = 8.9 mM.

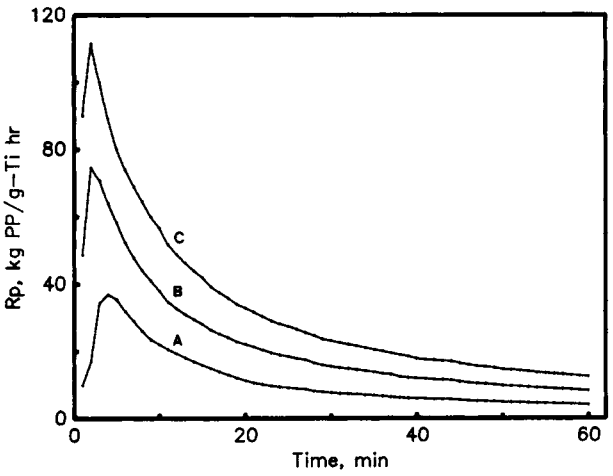

Figure 3 Polymerization profiles at $T = 50°C$, $[C_3H_6] = 0.43M$, $[AlEt_3] = 8.9\ mM$, and various amounts of catalyst: (A) Ti = 2.05×10^{-4} g; (B) 4.1×10^{-4} g; (C) 6.15×10^{-4} g.

2.0 and 2.9 times. According to the criterion for diffusion limitation in coordination polymerization,[11] the polymerization process may be diffusion-limited, if the initial rate of polymerization is proportional to the square root of catalyst concentration. The first-order dependence of catalyst concentration on the rate of polymerization in our polymerization system indicates that no diffusional limitation through the polymer film at the surface of the catalyst exists and that the amount of catalyst can be increased in our experimental conditions without causing the decrease of the monomer concentration in the liquid phase.

To determine the internal diffusion limitation in the porous catalyst, the Thiele modulus (Φ), characteristic of the ratio of an intrinsic polymerization rate in the absence of diffusion limitations to the rate of diffusion into the pore under polymerization conditions, was calculated according to following equation:

$$\Phi = \left(\frac{k_p C_0^*}{D_m}\right)^{1/2} S_0 \qquad (1)$$

where C_0^* is the initial concentration of active center; D_m, the diffusivity of propylene ($cm^2\ s^{-1}$); k_p, propagation rate constants ($M^{-1}\ s^{-1}$); and S_0, the initial radius of catalyst particle (cm). In a previous article,[8] we measured $k_p = 221\ M^{-1}\ s^{-1}$ when C^* was 0.26 mol/mol Ti at 50°C. The radius of the catalyst was measured with a scanning electron microscope. As shown in Figure 4, the catalyst is an agglomeration of subparticles, about 0.35 μm in diameter having an irregular shape. When polymerization takes place, loosely bound subparticles become separated and the voids will be filled with polymer.[12,13] By using $D_m = 35 \times 10^{-6}\ cm^2\ s^{-1}$ from published data[14] and S_0 from the SEM picture, we

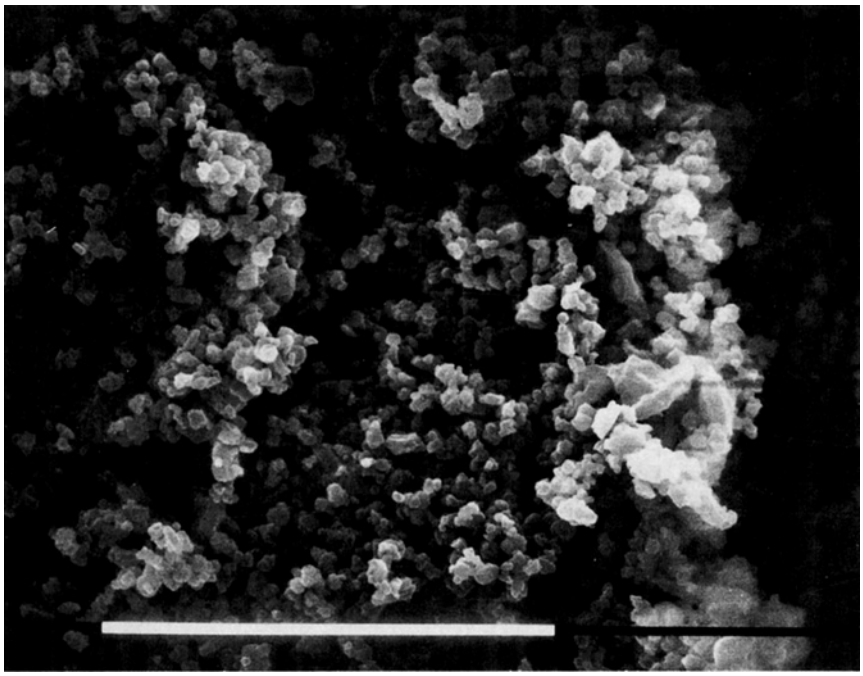

Figure 4 Scanning electron micrograph of the catalyst (magnification = ×6000).

obtained a value of $\Phi = 4.96 \times 10^{-4}$. This value of Φ is much smaller than unity and also smaller than that of α-$TiCl_3/AlEt_3$ (1.5×10^{-2}) and that of $(C_7H_7)_3TiCl/Mg(OH)Cl$ (3.3×10^{-2}) for propylene polymerization reported by other authors,[14] indicating that this catalytic system is not affected by the internal diffusion limitation. As a result, a kinetic analysis of propylene polymerization was carried out under the experimental conditions where the internal and the external diffusion limitation do not affect the intrinsic kinetic polymerization rate.

Effect of Monomer Concentration

The effect of monomer concentration on the rate of polymerization is shown in Figure 5. The maximum rate of polymerization, $R_{p,m}$ was obtained immediately upon the addition of the catalyst. Figure 6 shows that the polymerization rates at 3, 20, 60, and 90 min of polymerization at different monomer concentrations are directly proportional to the monomer concentration. Since we have identified the first-order dependency of R_p on the concentration of catalyst from Figure 3, the results of Figure 6 can be expressed as

$$R_p = k_p[C^*][M]$$

throughout the course of polymerization, where $[C^*]$ is the active site concentration of the catalyst.

Effect of Aluminum Alkyl Cocatalyst

The Al alkyl strongly affects the propylene polymerization kinetics and polymer stereoregularity.

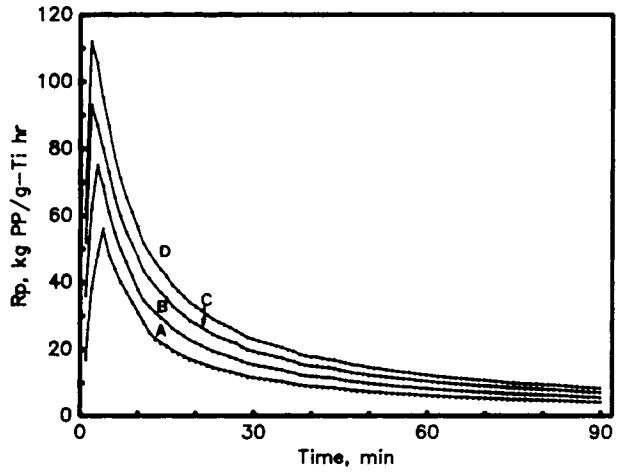

Figure 5 Polymerization rate profiles at $T = 50°C$, Ti $= 4.1 \times 10^{-4}$ g, $[AlEt_3] = 8.9$ mM, and various $[C_3H_6]$ of (A) 0.32, (B) 0.43, (C) 0.53, and (D) 0.60 M.

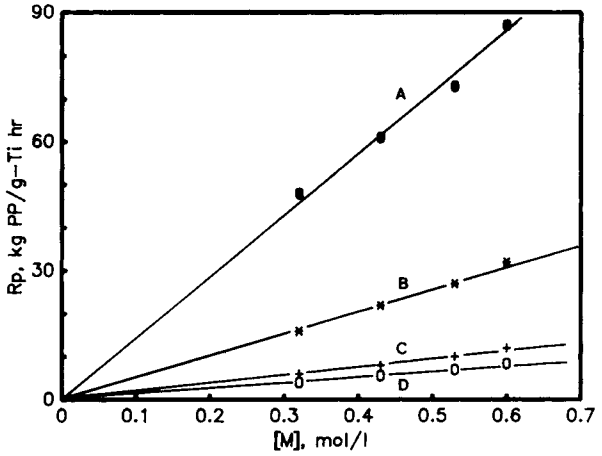

Figure 6 Dependence of polymerization rate on the monomer concentration. Polymerization conditions are the same as those indicated in Figure 5. Polymerization time: (A) 3 min; (B) 20 min; (C) 60 min; (D) 90 min.

The kinetic behavior, however, is difficult to generalize, since different results have been reported according to the olefin and the catalyst used.[15] In this sense, we investigated a detailed rate–time profile according to the concentration of Al alkyl and the result is shown in Figure 7. The rate of polymerization drops considerably after reaching maximum as the concentration of $AlEt_3$ increases. At all Al/Ti ratios, $R_{p,m}$ was reached in 1 or 2 min. Then, R_p decreased rapidly to a slow steady rate where the polymerization rate is about one-third to one-sixth of $R_{p,m}$ within 30 min. The similar kinetic behavior was also observed for the typical highly active catalyst of Mitsui-Montedison type.[16,17]

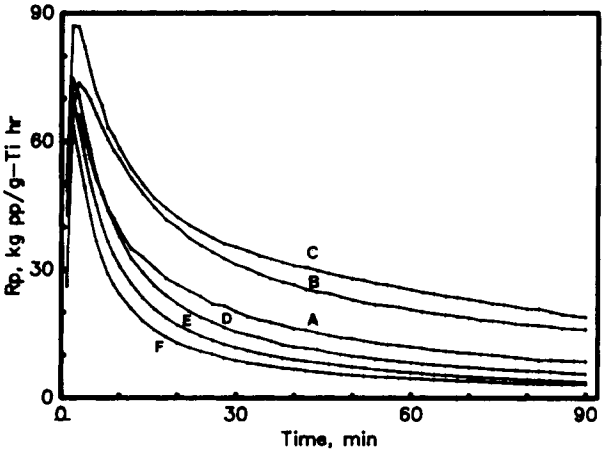

Figure 7 Polymerization rate profiles as a function of the concentration of $AlEt_3$ at $T = 50°C$, Ti $= 4.1 \times 10^{-4}$ g, $[C_3H_6] = 0.43$ M: (A) 1.12; (B) 2.23; (C) 3.35; (D) 8.9; (E) 20.1; (F) 42.4 mM.

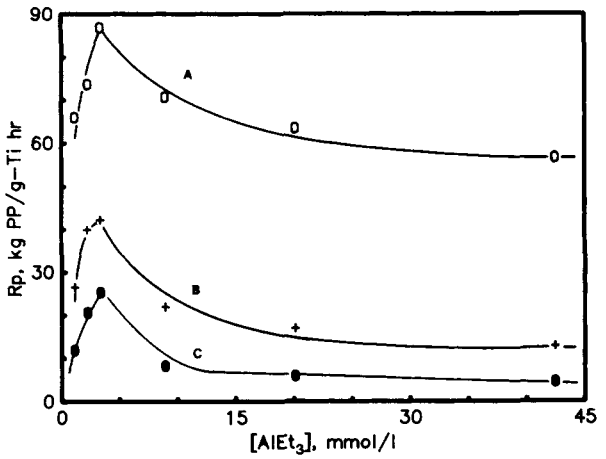

Figure 8 Dependence of polymerization rate on the concentration of $AlEt_3$. Polymerization conditions are the same as those indicated in Figure 7. Polymerization time: (A) 3 min; (B) 20 min; (C) 60 min.

The dependence of the polymerization rate on the concentration of $AlEt_3$ at various polymerization times is shown in Figure 8. A maximum rate of polymerization was observed at an Al/Ti ratio of approximately 20. In the case of the $TiCl_4/EB/MgCl_2$ catalyst, according to Spitz et al.,[18] the activity initially increases with the $AlEt_3$ concentration and then remains constant, tending to decrease only at very high $AlEt_3$ concentrations. On the other hand, other authors[15-17,19-21] reported a marked maximum in the activity vs. $AlEt_3$ concentration relationship. Depending on the catalyst system, maximum activity occurred at the ratio of Al/Ti between 10 and 50.

The average rate over 90 min of polymerization showed a similar maximum behavior as shown in Figure 9, i.e., the maximum average rate occurred at the Al/Ti ratio of about 20. In the case of propylene, isotacticity as well as kinetics are influenced by the nature and concentration of the Al alkyl. As observed by many authors,[15,22-24] besides activity, the isotacticity is also higher with $AlEt_3$ than with $AlEt_2Cl$, contrary to what happens with a conventional catalyst. Isotacities obtained with the present catalyst system decrease with increase of $AlEt_3$ concentration, similar to the case of typical $TiCl_4/EB/MgCl_2$ catalyst,[3,17] as shown in Figure 9.

Several kinetic models based on a number of plausible mechanisms of propagation and chain transfer have been suggested to interpret experimentally observed phenomena in propylene polymerization.[25] Langmuir–Hinshelwood rate laws have been applied in the kinetic analysis of Ziegler–Natta polymerization by Vasseley for propylene polymerization with $TiCl_3$—$AlEt_3$.[26] According to this model, chain propagation occurs by the insertion of an adsorbed monomer molecule at the propagation center. When the base metal is the polymerization center,

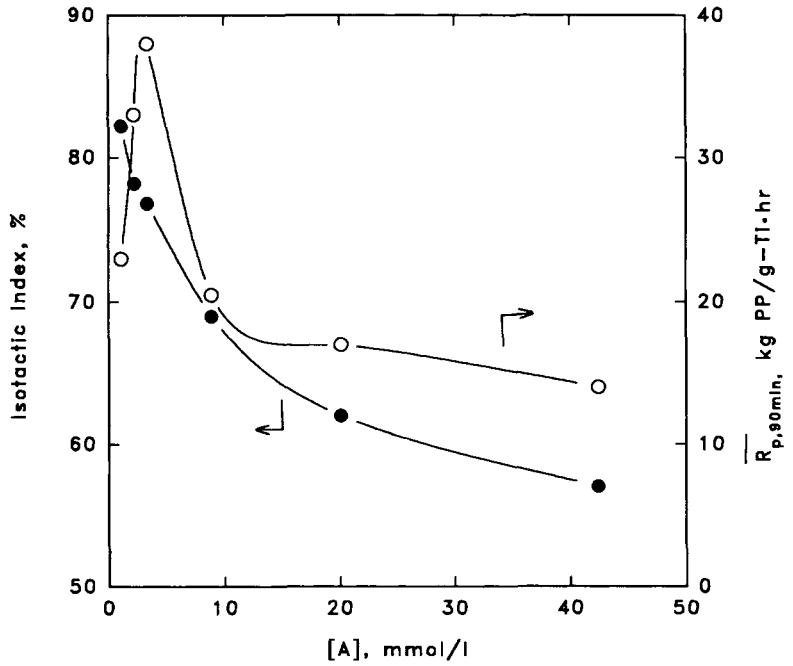

Figure 9 Dependence of average rate of polymerization (90 min) and isotacticity on the concentration of $AlEt_3$.

both aluminum alkyl and the monomer compete for the active sites on the catalyst surface. Adsorption of monomer and aluminum alkyl can be described by the Langmuir adsorption isotherms as follows:

$$\theta_M = K_M[M]/(1 + K_A[A] + K_M[M]) \quad (2)$$

$$\theta_A = K_A[A]/(1 + K_A[A] + K_M[M]) \quad (3)$$

where $[M]$ and $[A]$ represent the bulk concentrations of monomer and aluminum alkyl, respectively, and K_M and K_A are equilibrium constants for the corresponding adsorption equilibria. Then, the stationary propagation rate per unit mass of a transition-metal compound becomes

$$R_p = k_p\theta_A\theta_M = k_pK_AK_M[A][M]/(1 + K_A[A] + K_M[M])^2 \quad (4)$$

In eq. (4), it is assumed that the adsorption sites of both molecules are the same. At high $[A]$, $1 + K_A[A] \gg K_M[M]$, and eq. (4) reduces to

$$R_p = k_pK_AK_M[A][M]/(1 + K_A[A])^2 \quad (5)$$

Even if eq. (5) is an approximate form of eq. (4), the identical rate expression can be obtained by assuming that propagation proceeds by the reaction of a solute monomer with adsorbed aluminum alkyl dimer molecules and a vacant site.

According to the results obtained by Keii et al.,[17] the form of rate expression is independent of the polymerization time at which the rate equation is determined, except for the value of the apparent rate constant, $k(t)$. Then, eq. (5) can be written as

$$R_{p,t} = k(t)[M]K_A[A]/(1 + K_A[A])^2 \quad (6)$$

This suggests that the rate decay is independent of monomer and alkyl aluminum. Keii et al. confirmed the linear form of eq. (6) for $MgCl_2$-supported $TiCl_4$/EB catalyst, activated by $AlEt_3$.[17] Upon applying eq. (6) to the data shown in Figure 8, linear plots were obtained within the experimental error range (Fig. 10). The K_A values estimated from Figure 10 at 3, 20, and 60 min of polymerization times are 180, 190, and 210 M^{-1}, respectively, and the $k(t)$ values are 4.59×10^{-3}, 1.27×10^{-3}, and 6.63×10^{-4} s^{-1}, respectively. These results show that the decrease in the $k(t)$ value is mainly responsible for the rapid decrease of the polymerization rate during polymerization.

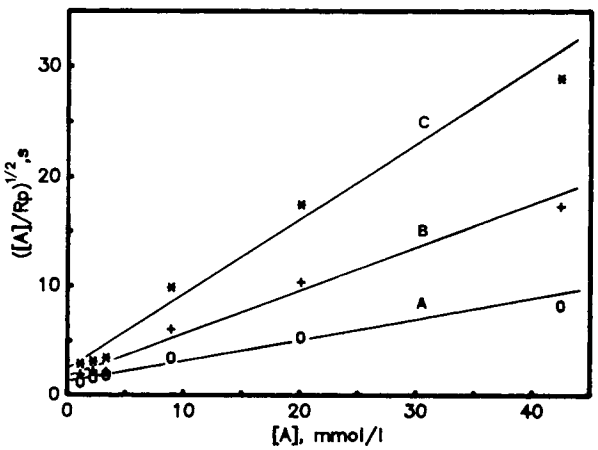

Figure 10 Langmuir–Hinshelwood plot for the data in Figure 8. Polymerization time: (A) 3 min; (B) 20 min; (C) 60 min.

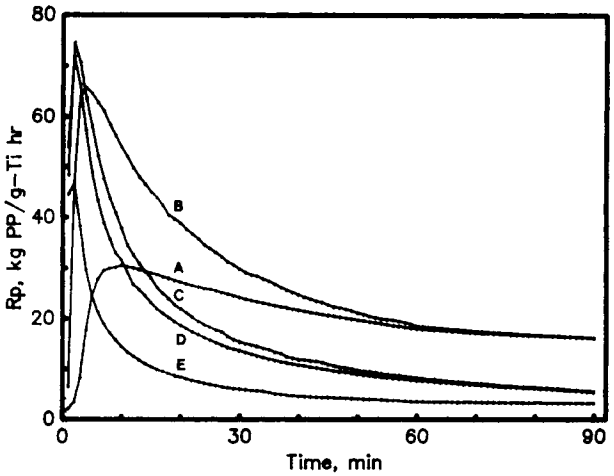

Figure 11 Polymerization rate profiles at Ti = 4.1×10^{-4} g, $[C_3H_6] = 0.43M$, $[AlEt_3] = 8.9$ mM, and various temperatures: (A) 25°C; (B) 40°C; (C) 50°C; (D) 60°C; (E) 70°C.

Effect of Temperature

The effect of temperature on the rate of propylene polymerization is shown in Figure 11. The maximum average rate of polymerization occurs around 40°C due to the much faster decay above 50°C. Because of catalyst deactivation, the polymerization rate declines rapidly during the early stage of polymerization; thus, the average rate (R_p) is somewhat dependent on the duration of polymerization. From the average rate over 90 min polymerization, the overall activation energy was estimated to be 8.5 kcal/mol at $T < 42$°C and −4.0 kcal/mol at T

> 42°C from the Arrhenius plot as shown in Figure 12. Keii et al. estimated the overall activation energy for the propylene polymerization with $MgCl_2$-supported $TiCl_4$/EB catalyst, activated by $AlEt_3$, to be 11.95 kcal/mol at $T < 41$°C and −5 kcal/mol at $T > 41$°C.[17] A similar temperature dependence has also been observed for ethylene polymerization with $TiCl_3/AlEt_2Cl$ (Ref. 27) and propylene polymerization with $TiCl_3/AlEt_3$.[28] For the propylene polymerization with $TiCl_4$/EB/$MgCl_2$, the catalyst activity showed a maximum near 60°C and then decreased with increasing temperature.[18,29,30] The decrease in the polymerization rate has been proposed to be irreversible in nature and, thus, in principle, can be ascribed to an irreversible deactivation of the active sites. Nevertheless, other explanations are possible. Berger and Grieveson[27] recognized a change of kinetics from $R_p \propto P$ (ethylene pressure) at lower temperatures, at which the activation energy is high, to $R_p \propto P^2$ at higher temperatures where the activation energy is low and proposed that a change of the rate-determining step from a chemical reaction at lower temperatures to a monomer diffusion at higher temperatures. Keii et al.[17] proposed another explanation for the observed dependence of the polymerization rate on the temperature. According to the usual adsorption kinetics, the constants $k(t)$ and K_A from eq. (6) can be expressed as follows:

$$k(t) = k(t)^0 \exp(-E/RT) \tag{7}$$

$$K_A = K_A^0 \exp(-E_A/RT) \tag{8}$$

where E is the activation energy of $k(t)$ and E_A is the adsorption energy of $AlEt_3$. Keii et al. approximated eq. (6) as

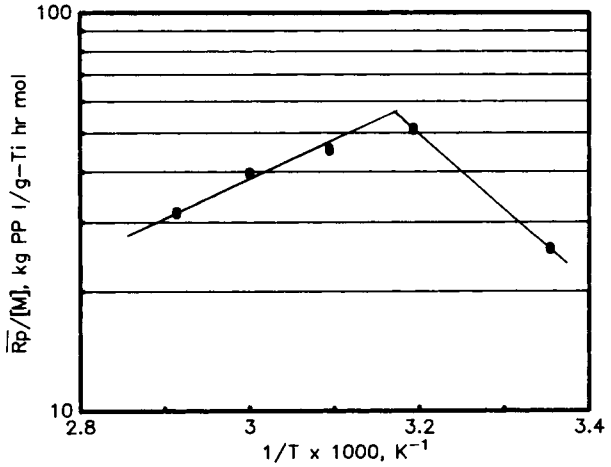

Figure 12 Arrhenius plot of $R_p/[M]$ vs. $1/T$.

$$R_p \propto k(t)[M]/K_A[A] \tag{9}$$

when $K_A[A] \gg 1$ at lower temperatures and

$$R_p \propto k(t)[M]K_A[A] \tag{10}$$

when $K_A[A] \ll 1$ at higher temperatures. Then, the overall activation energy E_{ov} at lower temperatures is

$$E_{ov} = E + E_A \tag{11}$$

whereas at higher temperatures,

$$E_{ov} = E - E_A \tag{12}$$

Applying these relations to the experimental results, we find

$$E = 2.2 \text{ kcal/mol and } E_A = 6.3 \text{ kcal/mol} \tag{13}$$

The values of E and E_A obtained by Keii et al.[17] for the $MgCl_2$-supported $TiCl_4$/EB catalyst were 3.6 and 8.6 kcal/mol, respectively. The optimum temperature at which the polymerization rate is maximum, i.e., $E_{ov} = 0$, can be calculated as follows: Using eq. (6), we have

$$E_{ov} = RT^2 d[\ln(R_p/[M])]/dT$$
$$= E - E_A(1 - 2\theta_A) = 0 \tag{14}$$

with $\theta_A = K_A[A]/(1 + K_A[A])$.

The value of θ_A at the optimum temperature is equal to 0.325 using the experimental values of E and E_A. The above results demonstrate that the adsorption energy of $AlEt_3$ is a contribution to the overall activation energy.

Effect of External Electron Donor

It is well known that the addition of various types of external electron donors in amounts less than that of the organoaluminum compounds to the catalyst system improves the isotacticity for propylene polymerization.[1-3,15] However, the improvement of isotacticity is marginal and there can be an adverse reduction in the polymerization rate. It is possible to produce a catalyst system capable of high isotacticity without losing its high activity by balancing the ability of external Lewis base to modify the ratio of the number of the isotactic site to that of the atactic site.[1-3]

The effect of the external donor, PEEB, on the polymerization rate is shown in Figure 13. As the ratio of the concentration of PEEB to that of $AlEt_3$ increases, the maximum R_p decreases. However, the rate of deactivation becomes slow when the small amount of PEEB is present in the polymerization medium. Accordingly, the average polymerization rate over 90 min of polymerization increases slightly when small amount of PEEB ($[PEEB]/[AlEt_3] = 0.1$–0.2) is used as a coactivator as shown in Figure 14. Both maximum R_p and average $\overline{R_p}$ decrease sharply when the ratios of $AlEt_3$ to PEEB are 0.3 and 0.5. The increase of $\overline{R_p}$ at the expense of $R_{p,m}$ at the small ratios of $[PEEB]/[AlEt_3]$ may be understood in terms of the complexation between $AlEt_3$ and PEEB, which will reduce the complexation of EB (internal donor) with $AlEt_3$. Hence, the dissociation of catalytic active species into inactive species or atactic active species may be retarded. Therefore, the catalytic activity remains more stable during polymerization. On the other hand, $R_{p,m}$ becomes smaller, probably because of the smaller number of active sites or the slower activation reaction due to the complexation of $AlEt_3$ with PEEB. Further increase in the $[PEEB]/[AlEt_3]$ ratio decreases $R_{p,m}$ and $\overline{R_p}$, because uncomplexed PEEB is a strong poison to active sites.

As expected, Figure 14 shows a significant increase in isotactic index by adding a small amount of PEEB. Busico et al.[31] Soga and Shiono,[32] and Kim et al.[7] showed that the internal Lewis base (EB) is readily removed by $AlEt_3$ when polymerization is carried out in the absence of external Lewis base.

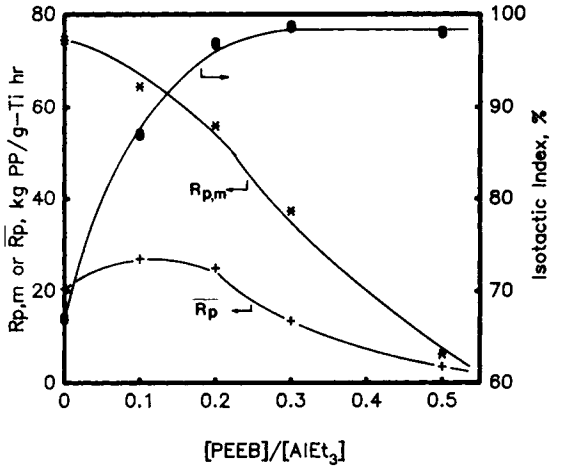

Figure 14 Maximum and average polymerization rate and isotactic indices at the various concentrations of PEEB.

As a result, the isotacticity of the polymer decreased drastically with an increase in the polymerization time. It is interesting to point out that the relevant isotacticity of the polymer is constant during polymerization when the amount of PEEB is one-fifth of $AlEt_3$ (Fig. 15). Busico et al.[31] interpreted the enhancement of isotacticity by two types of Lewis base: the internal base, which is one component of the solid catalyst, and the external base, which is one component of the cocatalyst solution, based on a plausible model of catalytic sites. According to this model, there may exist two types of Ti^{+3} species on the (100) surface of $MgCl_2$ in the absence of an internal donor: One is a mononuclear species having

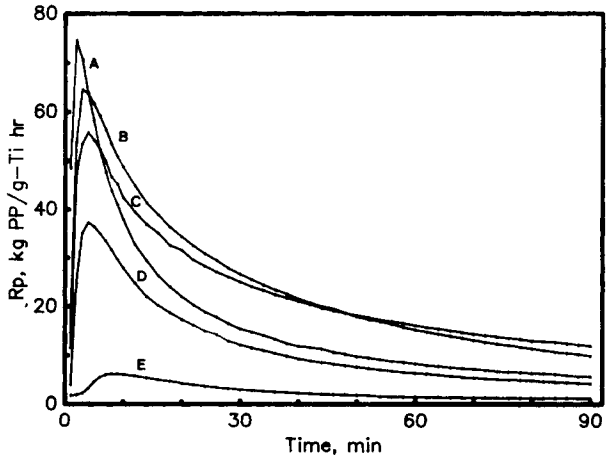

Figure 13 Polymerization rate profiles at $T = 50°C$, Ti $= 4.1 \times 10^{-4}$ g, $[C_3H_6] = 0.43M$, $[AlEt_3] = 8.9$ mM, and various [PEEB] of (A) $[PEEB]/[AlEt_3] = 0$, (B) 0.1, (C) 0.2; (D) 0.3; (E) 0.5.

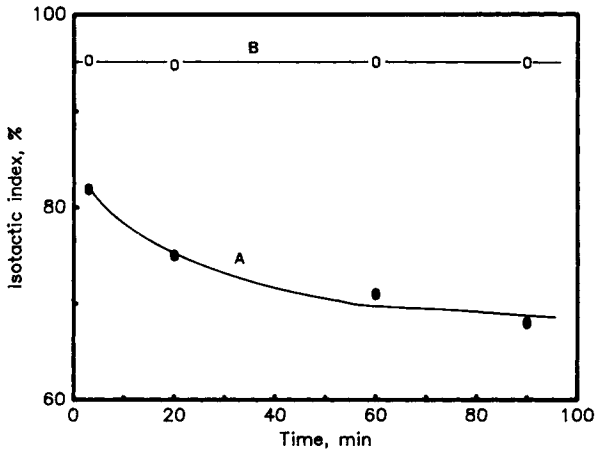

Figure 15 Relationship between isotactic index and polymerization time: (A) when $[PEEB]/[AlEt_3] = 0$; (B) when $[PEEB]/[AlEt_3] = 0.2$.

two vacant sites and the other is a binuclear species having one vacant site. Isotacticity is dictated by nonbonded interactions of the monomer at the catalytic center. They proposed that, contrary to the centers resulting from the mononuclear $TiCl_3$ complex, catalytic centers derived from chiral Ti_2Cl_6 dimers on the (100) faces of $MgCl_2$ crystals can have stereoregulating ability. If $AlEt_3$ and the external base are used together to activate the catalyst, the following equilibria may be considered based on the proposal by Busico et al.[28]:

$$Ti_2Cl_6 + \square \rightleftarrows 2TiCl_3 \quad (15)$$

$$\square + B(sol) \rightleftarrows B(ads) \quad (16)$$

$$2TiCl_3 + B(sol) \rightleftarrows Ti_2Cl_6 + B(ads) \quad (17)$$

where $TiCl_3$ is mononuclear surface complex; Ti_2Cl_6, a dinuclear complex; B(sol), the Lewis base in solution; B(ads), the Lewis base adsorbed on $MgCl_2$ surface; and □, the empty Mg coordination site.

Since the coordination of B and $AlEt_3$ seems not to be very strong, B should be partly eliminated during polymerization to generate a mononuclear surface complex. Therefore, equilibrium (15) may be established. If external donor, PEEB, is present in the polymerization medium, empty Mg coordination sites may be blocked, and, consequently, equilibrium (16) takes place. As a result, equilibrium (17) is shifted toward the formation of dinuclear centers by PEEB that blocks empty Mg coordination sites on the $MgCl_2$ surface. The steady isotactic index with polymerization time in the presence of PEEB may be explained by this proposal.

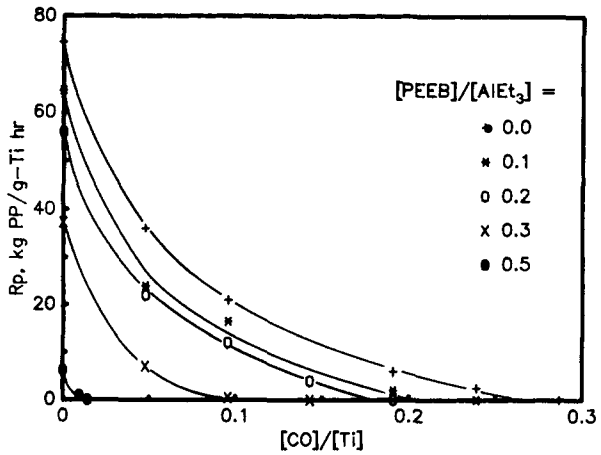

Figure 16 Relationship between the polymerization rate and the amount of CO added at $R_{p,m}$. Polymerization conditions are the same as those indicated in Figure 13.

Table I No. Active Sites, C^*, and the Propagating Rate Constant, k_p, in the Polymerization of Propylene with Different [PEEB]/[$AlEt_3$] Ratios

[PEEB] [$AlEt_3$]	R_{p-m} (kg PP/g − Ti h)	I.I. (%)	$10^2 \times C^*$ (mol/mol Ti)	k_p (L/mol s)
0	74.6	67.2	26	221
0.1	64.6	87.3	21	227
0.2	55.9	96.2	18	229
0.3	37.3	98.2	10	118
0.5	6.2	98.1	2	109

To elucidate the kinetic feature of the active sites in the presence of PEEB as coactivator, an attempt was made to determine the number of active centers C^* at the maximum rate by the CO inhibition method and the propagation rate constant k_p.[9,33] The dependence of the residual rate on the amount of CO introduced is shown in Figure 16. Assuming that an active site reacts with one molecule of CO, we measured the number of active sites from the minimum amount of CO consumed to stop the polymerization. The results are summarized in Table I, together with k_p values calculated from the relation $R_p = k_p C^* [M]$, with the observed values of C^*. The C^* value decreases from 0.26 at [PEEB]/[$AlEt_3$] = 0.0 to 0.18 at [PEEB]/[$AlEt_3$] = 0.2, whereas the k_p value remains unchanged within experimental error. Considering the increase in the isotactic index at the expense of the C^* value, PEEB increases the

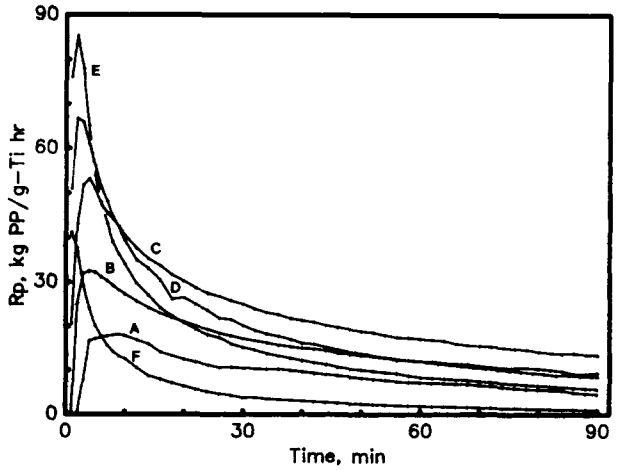

Figure 17 Polymerization rate profiles at Ti = 4.1 × 10^{-4} g, [C_3H_6] = 0.43M, [$AlEt_3$] = 8.9 mM, [PEEB]/[$AlEt_3$] = 0.2, and various temperatures of (A) 20°C, (B) 30°C, (C) 40°C, (D) 50°C, (E) 60°C, and (F) 70°C.

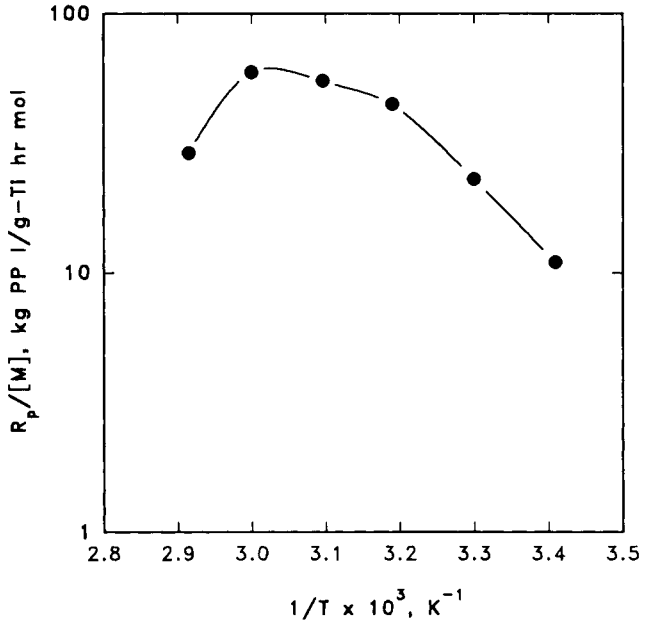

Figure 18 Arrhenius plot of $R_p/[M]$ vs. $1/T$.

catalyst isospecificity mainly by the selective poisoning of the sterically less hindered atactic active site rather than by an increase in the number of isospecific active sites.[34] A decrease in both the C^* value and the k_p value above a $[PEEB]/[AlEt_3]$ ratio of 0.3 demonstrates that PEEB in the polymerization medium deactivates not only atactic sites but also part of isospecific active sites.

The complicated effects of external donor on the catalyst affect the thermal stability of the catalyst. The kinetic curves of polymerization at different temperatures were obtained in the presence of PEEB (Fig. 17). When polymerization was conducted without using PEEB (Fig. 11), the maximum rate was obtained at 42°C. However, the temperature showing maximum activity was shifted to 60°C in the presence of PEEB. The Arrhenius plot of R_p averaged for 90 min polymerization vs. $1/T$ represents a smooth curve, as shown in Figure 18. The slope of the curve is steep, between 20 and 40°C, indicating that high temperature is needed to obtain high activity due to the fact that complicated equilibria (15)–(17) are difficult to form at low temperature, i.e., 20°C, by the presence of PEEB. Free PEEB not present in the formation of the equilibria at 20 or 30°C will hinder both nonisospecific and isospecific active sites. A relatively large amount of PEEB introduced participates in the establishment of equilibria (15)–(17), with a lesser amount of free PEEB remaining above 40°C. The complexed PEEB is thought to change nonisospecific sites to isospecific ones. The reactivity of PEEB does not change so much between 40 and 60°C; hence, the slope of the curve is gradual. A negatively steep slope above 60°C also shows that the thermal stability of active species formed by the presence of PEEB decreases sharply.

This research was partially funded by Honam Oil Refinery Co. and Research Center for Catalysis Technology (ERC) at POSTECH (1992). I.K. is also grateful to the Korea Research Foundation for the partial research fund (Non Directed Research Fund, 1992).

REFERENCES

1. F. J. Karol, *Catal. Rev.-Sci. Eng.*, **26,** 557 (1984).
2. K. Y. Choi and W. H. Ray, *J. Macromol. Sci. Rev. Macromol. Chem.*, **C25,** 1 (1985).
3. P. Galli, P. C. Barbe, and L. Noristi, *Angew. Makromol. Chem.*, **120,** 73 (1984).
4. N. Kashiwa et al., Br. Pat. 1,554,340, Mitsui Petrochem. Ind. (1979).
5. B. L. Goodall, U.S. Pat. 4,329,253, Shell Oil Co. (1982).
6. R. C. Job, U.S. Pat. 4,535,068, Shell Oil Co. (1985).
7. I. Kim, H. K. Choi, T. K. Han, and S. I. Woo, *J. Polym. Sci. Polym. Chem. Ed.*, **30,** 2263 (1992).
8. I. Kim and S. I. Woo, *Polym. Bull.*, **23,** 35 (1990).
9. I. Kim, J. H. Kim, and S. I. Woo, *J. Appl. Polym. Sci.*, **39,** 837 (1990).

10. S. Floyd, K. Y. Choi, T. W. Taylor, and W. H. Ray, *J. Appl. Polym. Sci.*, **31,** 2231 (1986).
11. L. L. Bohm, *Polymer,* **19,** 553 (1978).
12. C. W. Hock, *J. Polym. Sci. Part A-1,* **4,** 3055 (1966).
13. I. Kim and S. I. Woo, *Polym. J.*, **21,** 697 (1989).
14. J. C. W. Chien, *J. Polym. Sci. Polym. Chem. Ed.*, **17,** 2555 (1979).
15. P. C. Barbe, G. Cecchin, and L. Noristi, *Adv. Polym. Sci.*, **81,** 1 (1987).
16. J. C. W. Chien and C.-I. Kuo, *J. Polym. Sci. Polym. Chem. Ed.*, **23,** 731 (1985).
17. T. Keii, E. Suzuki, M. Tamura, M. Murata, and Y. Doi, *Makromol. Chem.*, **183,** 2265 (1982).
18. R. Spitz, J. L. Lacombe, and A. Guyot, *J. Polym. Sci. Polym. Chem. Ed.*, **22,** 2625 (1984).
19. P. Pino and B. Rotzinger, *Makromol. Chem. Suppl.*, **7,** 41 (1984).
20. S. Cai, H. Liu, H. Wang, and S. Xiao, *Cuihua Xuebao,* **3**(1), 7 (1982).
21. C. Dumas and C. C. Hsu, *J. Appl. Polym. Sci.*, **37,** 1605 (1989).
22. Y. Doi, E. Suzuki, and T. Keii, *Makromol. Chem. Rapid. Commun.*, **2,** 293 (1981).
23. J. A. Licchelli, R. N. Haward, I. W. Parsons, and A. D. Caunt, *Polymer,* **22,** 667 (1981).
24. A. Simon and A. Gröbler, *Transition Metal Catalyzed Polymerizations,* R. P. Quirk, Ed., MMI Press, Akron, 1983, p. 403.
25. Y. V. Kissin, *Isospecific Polymerization of Olefins,* Springer-Verlag, New York, 1985, p. 94.
26. K. Vesseley, *Pure Appl. Chem.*, **4,** 407 (1962).
27. M. N. Berger and B. M. Grieveson, *Makromol. Chem.*, **83,** 80 (1965).
28. T. Keii, K. Soga, K. Go, and M. Kojima, *J. Polym. Sci. Part C,* **23,** 453 (1968).
29. S. A. Sergeev, G. D. Bukatov, and V. A. Zakharov, *Makromol. Chem.*, **185,** 2 (1984).
30. J. C. W. Chien, C.-I. Kuo, and T. Ang, *J. Polym. Sci. Polym. Chem. Ed.*, **23,** 723 (1985).
31. V. Busico, P. Corradini, L. De Martino, A. Proto, and V. Savino, *Makromol. Chem.*, **186,** 1279 (1985).
32. K. Soga, T. Shiono, and Y. Doi, *Makromol. Chem.*, **189,** 1531 (1988).
33. A. D. Caunt, *Br. Polym. J.*, **12,** 22 (1981).
34. J. C. W. Chien and C.-I. Kuo, *J. Polym. Sci. Polym. Chem. Ed.*, **23,** 761 (1985).

Received March 3, 1993
Accepted December 17, 1993